Optimal parameter identification of linear and non-linear models for Li-Ion Battery Cells

Mohamed Assaad Hamida, Abdullah Shaheen, Ragab El-Sehiemy, Ehab Elattar

Optimal Parameter Identification of linear and non-linear models for Li-Ion Battery Cells

Abdullah M. Shaheen[1], , M A. Hamida [2], Ragab A. El-Sehiemy [3], Ehab E. Elattar[4]
[1] Electrical Engineering Department, Faculty of Engineering, Suez University
[2] Ecole Centrale de Nantes, LS2N UMR CNRS 6004, Nantes, France.
[3] Electrical Engineering Department, Faculty of Engineering, Kafrelsheikh University, Kafrelsheikh 33516, Egypt. [4] Electrical Engineering Department, College of Engineering, Taif University, P.O. Box 11099, Taif 21944, Saudi Arabia
Corresponding authors: mohamed.hamida@ec-nantes.fr; elsehiemy@eng.kfs.edu.eg

Abstract

This study proposes a reduced model based on the state space representation for identifying an accurate electric equivalent circuit of Lithium-Polymer Battery Cells. The parameter extraction process is formulated as non-linear optimization problem via three-stage procedure. The first stage estimates the state of charge (SoC) based on the non-linear characteristics associated with the battery current and the initial SoC condition. In the second stage, the open circuit voltage is estimated in terms of the resulted SoC that is employed in the first stage with varied linear and non-linear models. In the third stage, an Equilibrium Algorithm (EA), a recent optimizer, is developed for optimally identifying the battery parameters. The EA's parameters are adjusted based on Taguchi's design of experiment approach to reduce the computational time as well as the number of experiments that are required to get the optimum possible parameter arrangement. Numerical simulations associated with experimental implementation are emulated on Li-Ion Battery to prove the high capability of the proposed EA an as efficient identification procedure. In Addition, the proposed EA is characterized with high accuracy compared with several recent optimization algorithms for ARTEMIS driving cycle profile. The solution quality improvement of the proposed reduced model is achieved with high closeness to the experimental measurements for battery voltage and SoC. Furthermore, 16 % less computational times 12 % more accuracy are obtained by the proposed reduced model compared with linear and non-linear models.

Keywords: Li-Ion Battery Cells; Non-linear models;Equilibrium Optimizer; Three stage parameter identification; State of charge estimation.

List of Symbols and Nomenclature

SoC	State of charge
OCV	Open circuit voltage
EA	Equilibrium Algorithm
V_T	Battery terminal voltage
I_L	Battery terminal current
R_0	Internal resistance
Q_r	Nominal battery capacity
C_i	Equivalent circuit capacitors
R_i	Equivalent circuit resistances
V_{oc}	Open circuit voltage
V_{ex}	Experimental voltage
$F_i(u)$	is the objective function
$i$and u	is the estimated parameters of the battery
N	is the number of the estimated
u_{min}, u_{max}	are the accepted parameter bounds of control variable's vector u ,
$nobf$	is the number of objective functions.
$\hat{V}_{bat}$ and V_{bat}	refer to the estimated and experimental battery voltages, respectively.
w_1 and w_2	weighting factors to reflect the degree importance of objectives, F_1 and F_2.
min and max	refer to the minimum and maximum operators of the extracted parameters.
X^* and X	are the new and current vectors of the particle concentration, respectively.
$X_{r,eq}$	is a random extracted individual from the four best-so-far concentrations in equilibrium pool.
λ	The random factor and its range is within $[0, 1]$;
F	is an exponential term
Gr	is the rate of generation rate.

1. Introduction

1.1. Motivation

Energy storage systems act important role in facilitating the inclusion of different types of renewable resources such as wind, fuel and solar energies into the electrical power grids while the network reconfiguration is carried out with the existence of renewable distributed generation units [1]. Added to that, Energy storage can be used to manage the maximum load affecting on the power grids [2] as one of the important devices in the renewable energy resources [3]. Parameter estimation of battery is an urgent issue in recent years for efficient modeling of these elements on the overall system operation [4]. Finding the most accurate model for emulating the battery is still rich research field. Estimation of the battery parameters of various models is carried out based on the utilization of experimental methods. But this estimation procedure suffers from several demerits as cost expensive, high computational capacity, is needed in addition it consumes more time because the existence of repeated computation tasks In [5].

1.2. Literature Review

Several efforts have been employed for finding the optimal parameters of battery and to extract the state of charge. In [6],the parameters of the Lithium Ion Polymer are optimized by using the genetic optimization algorithm. In [7], another optimization method was developed by using the Simulated Annealing optimization method In [8]. The sunflower optimizer was developed for extracting the battery parameters and estimating the SoC of lithium ion battery. The proposed method is employed with aid of the state space model and the SoC with battery voltage relationship is represented by a linear equation which is not the case in reality. The model based methods are largely investigated especially for SoC estimation [9], [10]. An online extraction of the SoC based on the equivalent circuit with offer high accuracy and robustness [11]. A number of these methods includes parameters identification problem to deal in particular the internal resistance uncertainties. The authors in Ref. [9] proposes to use a Lunberger observer to estimate the SoC of Lithium-ion battery by considering the effect of the measurement noises on the parameter identification. The problem is solved by considering two linear models, the first one to estimate the SOC and the second one to identify the parameters. As it is well known, linear model can give an accurate estimation in limited operation conditions. Using the same approach, [12] proposed the real-time battery SoC is extracted based on the adaptive sliding observer. Firstly, an online parameter estimator was developed and then a sliding mode observer is designed based on the estimated parameters. The developed solution offers good results but it is very hard for real time implementation in particular when low cost embedded systems are employed. [13] propose to combined observer for parameter and SoC estimation. A H-infinity filter was employed for on-line parameter identification and a modified version of Kalman observer is employed for SoC estimation. Thanks to the online parameter identification, the proposed solution allows an accurate estimation of SoC in different operation conditions but the stability of the both observers cannot be guaranteed which limit its scope.

The electrochemical model was the crucial tool which allows to analyse the dynamic behaviour of lithium battery because it allows the analysis of the dynamic behavior of batteries [14]. Several SoC estimation methods have been implemented based on the electrochemical model, such that last-square fitting method, Kalman filtering and electromotive force method [15]. These methods offer an accuracy estimation in particular when the model impedance is updated. However, the estimation accuracy is affected by the aging of the battery and the related variations in the battery temperature.

The Open Circuit Voltage (OCV) was employed for estimating the SoC of lithium battery based on approximate linear relationship model to express the open circuit voltage in terms of the state of charge as presented in Refs. [16]. This relationship varies from a battery to another because it depends on the battery capacity and material. Moreover, it is not easy to express the OCV measurement in real time because that is needs cutting off the power and the battery rest for long period [17]. Another approach was considered for the estimation of the lithium battery SoC [18] on the basis of Ampere-hour counting method was also employed. This method offers an estimation in particular when the initial SoC is known. Moreover, the battery capacity should be not considered constant since it is affected with the battery lifetime [19]. The estimation of the Li-ion batteries SOC was the focus

of great number of researchers in recent 10 years. The dynamic model is considered with for formulating the parameters estimation problem. But, the rate of changes of the battery parameters is not considered in the previous studies of estimation process. The work in [20] discussed the change of rate of the estimated parameters. With the development of the computing systems, the intelligent mathematical tools become good candidate for SoC estimation of lithium battery system. Among these tools one can find neural network [21] fuzzy logic [22], adaptive neuro-fuzzy interface [23] and support vector machine [24].

These methods allow to meet the of accurate estimation requirements to represent the SoC independently to the battery internal circuit with the initial value of SoC by using the trained data and to work when the battery is operated in nonlinear conditions. The artificial intelligence method can be combined with other estimation methods such as model-based method as in [25] where a neural network is combined with a nonlinear observer to obtain an accurate estimation of SoC. However, the artificial intelligence methods require large memory to store a large data which is not always possible. Reference [26] presented an evaluation and assessment model for batteries that were connected in series into the grid. The assessment system is developed on the basis of the operation data in real domain. In Ref. [27], the aging issue of battery assessment in real world was carried on incremental capacity analysis accomplished with neural network as a radial training mechanism. In Ref. [28] presented the electrochemical energy based on combined mechanism storage systems. References it was presented a survey about the electrical vehicle application in smart grid environments. Reference [29] presented Random Forest Classification Feature for Analysis and Model the Li-Ion batteries. In Ref. [30] the machine learning method was developed for identifying the aging of Li-Ion batteries as an assessment study.

The optimization techniques with their excellent global search abilities were used for the parameter identification and SoC estimation of lithium batteries [31]. These techniques presented excellent tools to identify with high accuracy the parameters of the developed battery models. The optimization algorithms are generally combined with other estimation tools such as genetic algorithm [32], model-based method [31], battery equivalent circuit method [33]. The estimation obtained by using the optimization algorithms depend also on the employed model. The using of the nonlinear models lead to more accuracy estimation [34] compared to the linear models. However, the nonlinear models are more complicated and require more computing time even when the battery is operated in linear conditions. Recently, the equilibrium optimization algorithm was proposed by A. Faramarzi et al. in [35]. The EA has a straightforward optimization framework with adaptive controlling parameters. It simulates the dynamic equilibrium states that describe and characterize the mass balance patterns. In the EA, each search individual mimics the concentration of a particle which is randomly initialized and updated in respect of attaining the optimal fitness that mimics the final equilibrium state. Later, some EA applications are noticed in the literature for solving engineering problems of image segmentation [36], vehicle components design [37], parameters extracting of fuel cell [38], and economic dispatch [39]. As further successful applications of EA the following references can cited: distributed generation (DG) allocation with network reconfiguration [40], Feature Selection [41], Optimal Power Flow (OPF) of hybrid grids [42], OPF with Renewable Energy [43], and biomass DGs placement in power systems [44].

1.3. Research Gap

Many issues are considered for modeling the battery parameters identification and SOC estimation. Actually, no assessment for the impact non-linear modeling were considered the previous studies in the literature. Also, most of the models presented in the literature are based on a complex state space model. The linear model doesn't need lot of computation time for parameter identification. However, it can not give a good accuracy for parameter identification because the Lion-Ion Battery is a nonlinear system. From the other side, nonlinear model can give a good accuracy for parameter estimation, but it requires longer computation time. The proposed strategy has produced a reduced nonlinear model which give a good identification accuracy with less computation time compared to classical nonlinear models. Then, the parameter estimation are greatly effected by the solution method. To overcome this problem, the proposal of the reduced model with enough accuracy for parameter estimation becomes an absolute necessity The current study is concerned with the previous raised research gaps in the literature. In this regard, linear and non-linear representation of the relation between open circuit voltage and the state of charge are considered.

1.4. Paper Contributions

The salient features of this study are summarised as follows:

1. The state space model is divided into three separated models that enhance the solution methodology and find the accurate relation for each stage.
2. in this study, an assessment between the various linear and non-linear models, that are employed the relation between open circuit voltages and the battery state of charge.
3. An new solution methodology based on Enhanced Equilibrium Optimization Algorithm (EA) is proposed considering statistical indices that reflect the proposed method capability.
4. The EA's parameters are designed based on Taguchi's design of experiment approach.
5. The proposed procedure is initially applied on real Li-Ion Battery Characteristics then dynamic verification study is carried out on ARTEMIS driving cycle.
6. Less computational time is achieved by using the reduced model at acceptable level of accuracy compared with linear and non-linear models.

1.5. Paper Organization

The rest sections of this study are organised as follows: Section 2 presents the problem formulation of the considered parameters estimation problem of the Li-IOn battery. In Section 3, the proposed battery parameters and SoC estimation is introduced. The experimental results are presented in Section 4. This study conclusions are reported in Section 6.

2. Problem Formulation

The problem of battery parameters estimation is still of interest for many researchers . The proposed formulation describes the way to compute the battery voltage and state of charge. According to [8], the battery voltage and the state of estimation are modelled by state space model as:

2.1. Modeling of Lithium Ion Battery

The general equivalent circuit model is constructed with a number of n times RC elements denoted by nRC-model [45], normally it is extended up to 3 RC elements[46]. The RC group is considered as relaxation part to avoid the complexity raised for the extraction the battery parameters. In the sequel,the state space model for the battery dynamics is represented in the following form:

$$\begin{aligned} \dot{X} &= AX + Bu \quad (1) \\ y &= CX + Du + b_0 \quad (2) \end{aligned}$$

where,

$$X = \begin{bmatrix} SOC \\ V_{rc} \end{bmatrix},$$

$$A = \begin{bmatrix} 0 & 0 \\ 0 & -\frac{1}{RC} \end{bmatrix}, B = \begin{bmatrix} \frac{1}{Q_R} \\ \frac{1}{C} \end{bmatrix}, C = \begin{bmatrix} b_1 & 1 \end{bmatrix}, D = R_0.$$

To describe the static characteristic of the battery under predetermined conditions of temperature and age, Equation (3) presents a linear relationship between the V_{oc} and SoC is assumed as [47] as:

$$V_{OC} = f(SOC) = b_0 + b_1 SOC. \quad (3)$$

The nonlinear relation that describes the open circuit voltage versus the state of charge can be expressed in exponential form as:

$$\begin{aligned} V_{OC} &= f(SOC) = a_O + \sum_{i=1}^{N} a_j e^{a_{j+1}(1-SOC)^i} \\ &\quad + a_{j+2} e^{a_{j+3}(SOC)^i} \quad (4) \end{aligned}$$

where

$$j = i + 3 \times (i - 1)$$

Based on Eq. (4), the variable N can control the number of terms that is used to describe the nonlinear relation between V_{OC} and SOC.

In the current work,the state space dynamic model is used to describe the terminal voltage (V_T) versus current (I_L). Both the temperature and ageing of the battery effects are not considered in this work.

2.2. Parameterization model development

To optimize the parameters of the Li-ion battery model, The dynamic model of the battery described in the previous section is used. An objective function has to be set for fitting the estimated output voltages with the corresponding recorded voltage in the experimental tests. This objective function aims at minimizing the Squares Error Sum (SSE) between the estimated and experimental data. The common form of this optimization form is:

$$\begin{aligned} min_u F_i(u), i = 1, 2..nobf \\ u_{min} \leq u \leq u_{max} \end{aligned} \tag{5}$$

The parameters extraction model is dependent on the battery experimental data. In the proposed method, two cases studied are considered. A multi-objective MoF fittness function that aims at minimizing the aggregation of the root mean square of the normalized deviation between both the estimated and experimental battery voltage and the estimated and experimental state of charge is proposed. This function MoF combines two objectives which are:

$$F_1(u) = \sum (\frac{\hat{Vbat} - Vex}{V_{bat}^{max}})^2; \tag{6}$$

$$F_2(u) = \sum (\frac{\hat{SOC} - soc}{soc^{max}})^2; \tag{7}$$

The first objective function ($F_1(u)$) represents the normalized deviation between extracted and experimental voltage of the battery while the second one represents the normalized deviation of the state of charge ($F_2(u)$). Then, the combined objective function of the battery model identification can be expressed as:

$$MoF(u) = w_1 \times \sum_{i=1}^{n} (\frac{\hat{Vbat} - Vex}{V_{bat}^{max}}) + w_2 \times \sum_{i=1}^{n} \mid (\frac{\hat{SOC} - soc}{soc^{max}}) \mid \tag{8}$$

Then, the combined objective function,Eq. (8), is optimized with respecting the following inequality constraints for each control parameter (u) within their boundaries as:

$$R_{min} \leq R \leq R_{max} \tag{9}$$

$$R_{0_{min}} \leq R_0 \leq R_{0_{max}} \tag{10}$$

$$C_{min} \leq C \leq C_{max} \tag{11}$$

$$b_{0_{min}} \leq b_0 \leq b_{0_{max}} \tag{12}$$

$$b_{1_{min}} \leq b_1 \leq b_{1_{max}} \tag{13}$$

$$Q_{r_{min}} \leq Q_r \leq Q_{r_{max}} \tag{14}$$

Table 1: The nonlinear relation between V_{OC} and SOC

N	Model $V_{OC} = f(SOC)$	Parameters	Number
1	$=\mathrm{a}_0 + a_1 e^{a_2(1-SOC)} + a_3 e^{a_4 SOC}$	a_0, a_1, ... a_4	5
2	$=\mathrm{a}_0 + a_1 e^{a_2(1-SOC)} + a_3 e^{a_4 SOC} + a_5 e^{a_6(1-SOC)^2} + a_7 e^{a_8 SOC^2}$	a_0, a_1, ... a_8	9
3	$= a_0 + a_1 e^{a_2(1-SOC)} + a_3 e^{a_4 SOC} + a_5 e^{a_6(1-SOC)^2} + a_7 e^{a_8 SOC^2}$ $+ a_9 e^{a_{10}(1-SOC)^3} + a_{11} e^{a_{12} SOC^3}$	a_o, a_1, ... a_{12}	13
4	$= a_O + +\mathrm{a}_1 \mathrm{e}^{\mathrm{a}_2(1-\mathrm{SOC})} + \mathrm{a}_3 \mathrm{e}^{\mathrm{a}_4 \mathrm{SOC}} + \mathrm{a}_5 \mathrm{e}^{\mathrm{a}_6(1-\mathrm{SOC})^2} + \mathrm{a}_7 \mathrm{e}^{\mathrm{a}_8 \mathrm{SOC}^2}$ $+ \mathrm{a}_9 \mathrm{e}^{\mathrm{a}_{10}(1-\mathrm{SOC})^3} + \mathrm{a}_{11} \mathrm{e}^{\mathrm{a}_{12} \mathrm{SOC}^3} + \mathrm{a}_{13} \mathrm{e}^{\mathrm{a}_{14}(1-\mathrm{SOC})^4} + \mathrm{a}_{15} \mathrm{e}^{\mathrm{a}_{16} \mathrm{SOC}^4}$	a_o, a_1, ... a_{16}	17
5	$= \mathrm{a}_\mathrm{o} + \mathrm{a}_1 \mathrm{e}^{\mathrm{a}_2(1-\mathrm{SOC})} + \mathrm{a}_3 \mathrm{e}^{\mathrm{a}_4 \mathrm{SOC}} + \mathrm{a}_5 \mathrm{e}^{\mathrm{a}_6(1-\mathrm{SOC})^2} + \mathrm{a}_7 \mathrm{e}^{\mathrm{a}_8 \mathrm{SOC}^2}$ $+ \mathrm{a}_9 \mathrm{e}^{\mathrm{a}_{10}(1-\mathrm{SOC})^3} + \mathrm{a}_{11} \mathrm{e}^{\mathrm{a}_{12} \mathrm{SOC}^3} + \mathrm{a}_{13} \mathrm{e}^{\mathrm{a}_{14}(1-\mathrm{SOC})^4} + \mathrm{a}_{15} \mathrm{e}^{\mathrm{a}_{16} \mathrm{SOC}^4}$ $+ \mathrm{a}_{17} \mathrm{e}^{\mathrm{a}_{18}(1-\mathrm{SOC})^5} + \mathrm{a}_{19} \mathrm{e}^{\mathrm{a}_{20} \mathrm{SOC}^5}$	a_o, a_1, ... a_{20}	21
6	$= \mathrm{a}_\mathrm{o} + \mathrm{a}_1 \mathrm{e}^{\mathrm{a}_2(1-\mathrm{SOC})} + \mathrm{a}_3 \mathrm{e}^{\mathrm{a}_4 \mathrm{SOC}} + \mathrm{a}_5 \mathrm{e}^{\mathrm{a}_6(1-\mathrm{SOC})^2} + \mathrm{a}_7 \mathrm{e}^{\mathrm{a}_8 \mathrm{SOC}^2}$ $+ \mathrm{a}_9 \mathrm{e}^{\mathrm{a}_{10}(1-\mathrm{SOC})^3} + \mathrm{a}_{11} \mathrm{e}^{\mathrm{a}_{12} \mathrm{SOC}^3} + \mathrm{a}_{13} \mathrm{e}^{\mathrm{a}_{14}(1-\mathrm{SOC})^4} + \mathrm{a}_{15} \mathrm{e}^{\mathrm{a}_{16} \mathrm{SOC}^4}$ $+ \mathrm{a}_{17} \mathrm{e}^{\mathrm{a}_{18}(1-\mathrm{SOC})^5} + \mathrm{a}_{19} \mathrm{e}^{\mathrm{a}_{20} \mathrm{SOC}^5 + \mathrm{a}_{21} \mathrm{e}^{\mathrm{a}_{22} \mathrm{SOC}^6 + + \mathrm{a}_{23} \mathrm{e}^{\mathrm{a}_{24} \mathrm{SOC}^7}}}$	a_o, a_1, ... a_{24}	25

3. Proposed Battery Parameters Procedure based EA

The parameter extraction problem is represented as non-linear three-stage procedure based optimization problem. The first stage estimates the SoC based on its non-linear relation defined by equations with the battery current (1)-(2) considering the initial SoC condition. It can be computed by equation(15). In this equation, η refers to the battery efficiency and SoC_{int} refers to the initial condition of the SoC. In the second stage, the open circuit voltage is estimated in terms of the resulted SoC that is employed in stage 1 with varied linear and non-linear models. Equation (4), represents these several models that describe the nonlinear relation between V_{OC} and SOC by varying the number of the control parameters that are required to be identified as reported in the Table 1. From this table, 6 non-linear models are used to express the open circuit voltage and SoC

$$SoC = 100\dot{(}SoC_{int} - \frac{1}{Q_n}\int \eta I_b dt) \tag{15}$$

In the third stage, the recent optimizer called equilibrium algorithm is employed for optimally identifying the battery parameters. In EA [35], the initial concentrations with a particular number (Npr) are iteratively generated

$$\mathrm{X}^* = \mathrm{X}_{\mathrm{r,eq}} + \frac{\mathrm{Gr}}{\lambda}(1-\mathrm{F}) + (\mathrm{X} - \mathrm{X}_{\mathrm{r,eq}}) \cdot \mathrm{F} \tag{16}$$

$$F = A_1 sign(B - 0.5).(e^{-\lambda(1-\frac{Z}{Z_{max}})^{A_2 Z/Z_{max}}} - 1) \tag{17}$$

$$\mathrm{Gr} = \begin{cases} 0.5\mathrm{r}_1\,(\mathrm{X}_{\mathrm{r,eq}} - \lambda \mathrm{X})\,\mathrm{F} & \text{if } \mathrm{r}_2 \geq \mathrm{GP} \\ 0 & \text{if } \mathrm{r}_2 < \mathrm{GP} \end{cases} \tag{18}$$

where, the constants A1 and A2 equal 2 and 1 , respectively. the vector B, r_1 and r_2 are is random within range [0, 1]; Z and Z_{max} are the current and the maximum number of the iterations, respectively. are random numbers within range $[0, 1]$; GP is the probability of generation that is set to 0.5. As shown (16), the updating process of each particle concentration is mainly based on the effect of three parts. The first is the extracted individual from the four best-so-far concentrations in the equilibrium pool. The second and third parts is dependent on the variation measure between the extracted equilibrium concentration and the current one. These two parts have a randomized vector of exponential behavior that is responsible for exploitation and exploration characteristics of the EA in the search space to optimally find the outcome. The main steps of the EA can be written as follows:

1. Create the initial population of the particle's concentrations randomly.
2. Check the bounds of the control variables (u) and set any violated one to its nearest bounds ((9)-(14)).
3. Estimate the fitness function in Equation (8) of each concentration in the population.
4. Pick out the four best-so-far concentrations to form the equilibrium pool using Equation(16).
5. Update the exponential term (F) and the generation rate (Gr) using Equations (17) and (18), respectively.
6. Update each particle concentration X^* using Eq. (16).
7. Go to step 2 until reaching the maximum iteration number which is considered as the stopping criteria.

4. Experimental Results

In this study, the 40 Ah Li-ion battery cell is an example of the commercial batteries that achieve high improvements in the drive performance and its accompanied reliability [48]. The pertinent specifications that can be found in the data -sheet are: nominal voltage equals 3.7 V, internal resistance is 0.9 mΩ, the capacity 40 Ah, specific energy is 167 Wh/kg of weight 0.885 kg and both charging/discharging currents are 40A. In this study, the proposed estimation procedure is employed for two cases. These cases are considered to emulate linear and non-linear representation for the relation between V_{OC} and SoC as follows:

1. Case study 1: Consideration of Linear relation between V_{OC} and SoC
2. Case study 2: Consideration of Non-Linear relation between V_{OC} and SoC

Added to these two cases, the proposed estimation procedure is developed for Artemis driving cycle.

Table 2: Bounds of battery parameters [8]

Variables	LB	UB	Variables	LB	UB
R (mΩ)	0.01	10	b_0(V)	1	5
C_1 (μF)	0	105	b_1 (V)	0	3
R_1 (Ω)	0	1300	a_0, a_1.....$a_2$4	-100	100
Q_R (As)	13000	170000			

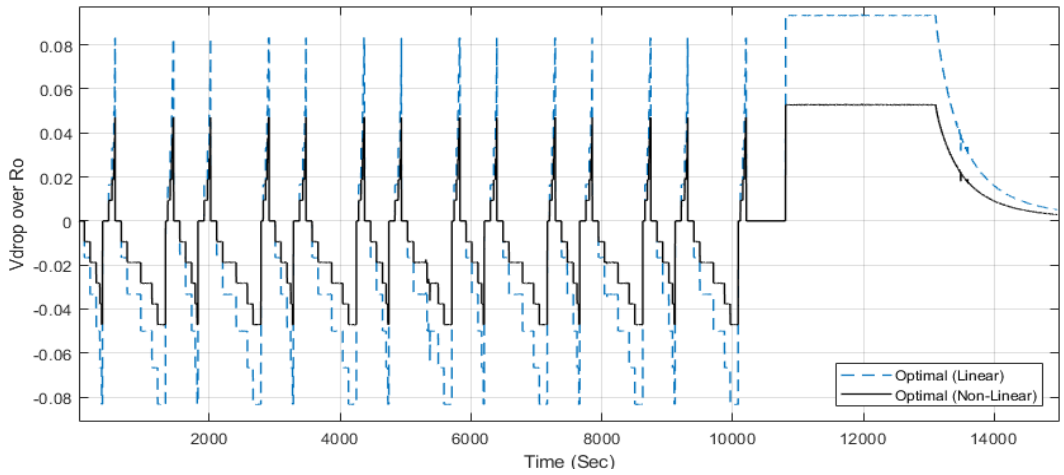

Figure 1: Response of the voltage drop over the internal resistance for ARTEMIS driving cycle

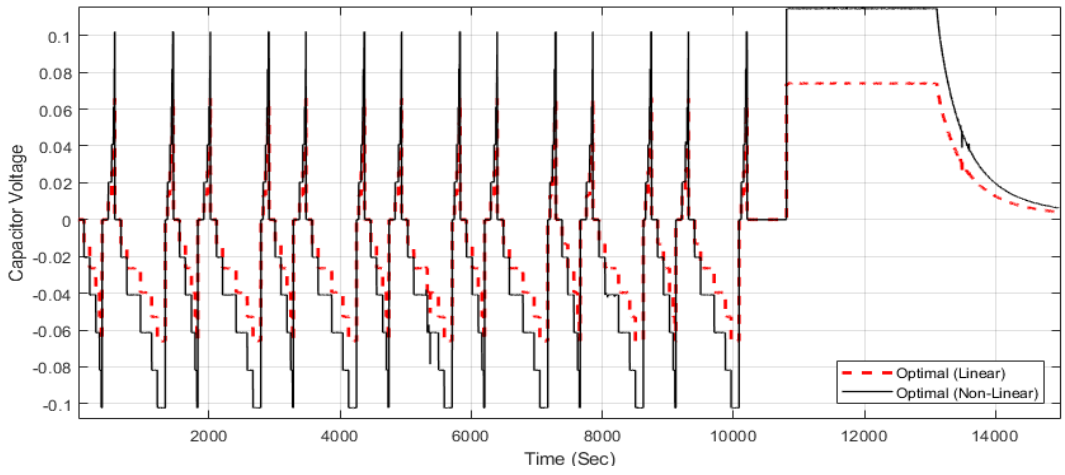

Figure 2: Response of the capacitor voltage for ARTEMIS driving cycle

4.1. Simulation results of Case study 1

Table 2 presented the considered boundaries of the estimated parameters of the battery cells. In the first case, the relation between V_{OC} and SOC is taken in its linear form as

Table 3: Optimal parameters based on EA for Linear and Non-linear Models

Parameter	Linear	Non-Linear	
R (mΩ)	0.13120618	0.000568	
R_1 (Ω)	0.74081781	0.000954	
C_1 (F)	0.0001026851	0.036197	
R_2 (Ω)	0.033796674	0.000946	
C_2 (F)	0.0022340423	0.059282	
Q_r (As)	144000	147964.2	
Coefficients	b_0 = 3.36673 b_1 = 0.74081	a_0=3.7480 a_1=0.3658 a_2=-3.0791 a_3=-0.2624 a_4=-14.4221 a_5=0.1348 a_6=-10.8373	a_7=-0.1236 a_8=-1.5833 a_9=-0.06919 a_{10}=0.7384 a_{11}=0.0228 a_{12}=-3.2842 a_{13}=-0.1626
F1	0.015985615	0.007243354	
F2	0.013588193	0.0004103893	
MOF	0.029239027	0.0076537439	

described in Eq. (3) [48]. The proposed EA is applied for minimizing the aggregation of the root mean square of the normalized difference between both battery voltage and state of charge for the experimental and estimated values. Table 3 shows the obtained optimal parameters and their corresponding results.

4.2. Simulation results of Case study 2

In the second case, the relation between V_{OC} and SOC is taken in its non-linear form as described in Eq. (4) [49]. Similar to Case 1, the proposed EA is applied effectively, and the optimal results is tabulated in Table 3. In this case, the identified parameters are more than double the parameters in Case 1. However, the considered objective, in this case, is greatly minimized to 0.00765 compared to 0.0292 in Case 1. Both indexes are minimized where the root mean square of the normalized difference of the battery voltage between both the estimated and experimental records is declined to 0.0072 and the estimated and experimental state of charge is declined to 0.0135 as well.

Fig. 3 depicts the estimated battery voltage versus the corresponding experimental voltage for Cases 1 and 2. Great improvement is shown in the estimated battery voltage in Case 2 compared to Case 1. This improvement is originally due the accurate high non-linearity consideration between the open circuit voltage and the state of charge as shown in Fig. 4. This figure clearly illustrates the curved relationship in Case 2 that makes accurate tracking to the experimental battery voltage. Fig. 5 depicts the estimated battery voltage versus the corresponding experimental voltage in both forms. As shown, great improvement

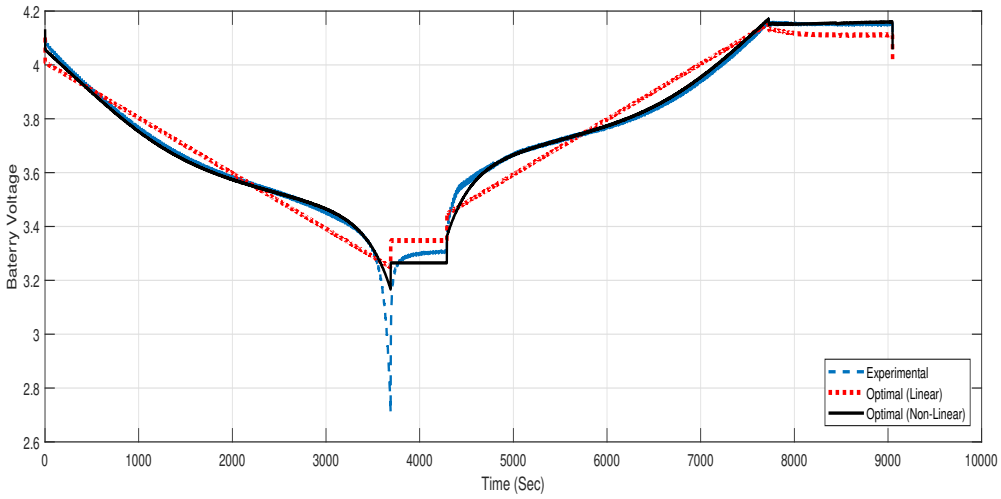

Figure 3: Constant current profile with CC/CV charge protocol (b) Experimental and modeling responses of battery voltage

in the estimated battery voltage in the non-linear model compared to the linear model. Not only that, but also great improvement in the estimated SOC in Case 2 compared to Case 1 is acquired as clearly shown in Fig. 6 that depicts the estimated SOC versus the experimental SOC for Cases 1 and 2.

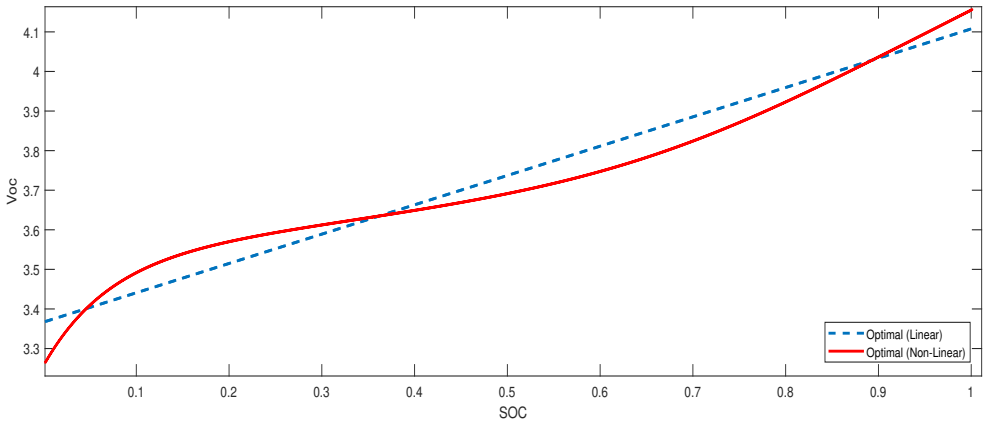

Figure 4: Relation between estimated open circuit voltage and SOC for Cases 1 and 2

4.3. Effect of exponential terms in the Non-Linear relation between V_{OC} and SOC

As discussed previously, the non-linear form that describes the relation between V_{OC} and SOC has better performance than the linear form. In this subsection, the effect of increasing

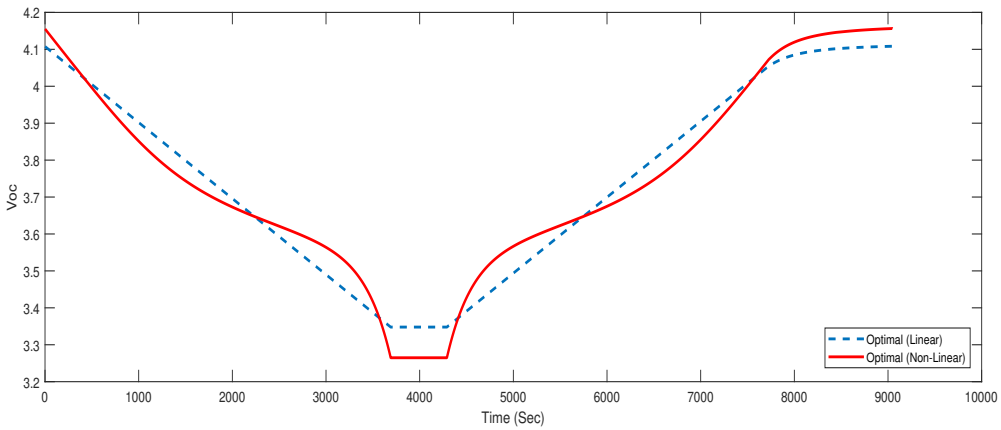

Figure 5: Responses of the estimated open circuit voltage for Cases 1 and 2

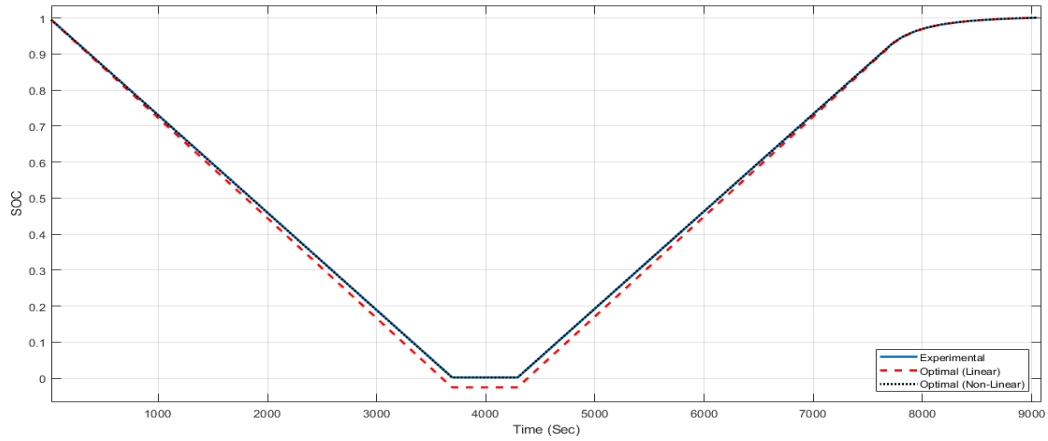

Figure 6: Experimental and modeling responses of battery SOC

and decreasing the exponential terms in the Non-Linear relation of Eq. (5) between V_{OC} and SOC is considered. This effect is discussed by controlling the number (N) in Eq. (5). Table 4 summarizes the optimal parameters based on EA for different N values which is specified at 5, 9, 13, 17, 21, and 25, respectively. The proposed EA can reach the minimum MOF in all cases of 0.00775, 0.00764, 0.00764, 0.00784, 0.00765, and 0.00767 at N values of 5, 9, 13, 17, 21, and 25, respectively. As shown, no significant improvement in the accuracy by increasing N values more than 9. On the other side, the more increasing of the value of N, the more increasing in the parameters that are required to be optimally identified. Consequently, the computational complexity is increased and so it needs more calculation time.

Table 4: Optimal parameters based on several algorithms for Case 2

N	5	9	13	17	21	25
R_0	0.000313	0.00092	0.00115	0.00025	0.00087	0.00058
a_0	3.44539	2.90216	2.95816	3.04743	3.86027	1.53556
a_1	0.71692	-0.01987	-0.25092	-0.17554	-0.11100	3.08155
a_2	-2.09764	-71.41551	-10.28074	-2.50577	-0.33987	-0.29232
a_3	-0.27755	-0.32546	-0.30660	-0.3110	-0.56280	0.01156
a_4	-15.19273	-12.19807	-13.39952	-15.64221	-5.86341	2.32518
a_5	23.26866	0.05772	0.06925	3.11795	-0.46976	0.00942
a_6		-11.4172	-1.91169	-5.23991	-5.11693	-26.91067
a_7		0.68162	0.40582	0.32992	0.35757	0.40626
a_8		0.5718143	1.22954	-6.09220	-20.68999	-2.88182
a_9		27.92645	-0.03106	-2.68465	2.18453	-0.07038
a_{10}			-82.95173	-14.23189	0.04824	1.58637
a_{11}			0.18982	0.19827	-1.74397	-0.04575
a_{12}			-2.43041	-1.04874	0.0047	0.23968
a_{13}			22.27915	0.75288	0.39776	-0.0105
a_{14}				-34.4296	-1.22888	3.63572
a_{15}				-0.01623	-1.05411	-0.03389
a_{16}				-6.10648	-2.00274	-0.37811
a_{17}				46.01661	0.18642	0.01262
a_{18}					-2.41969	0.08977
a_{19}					0.05885	-0.1899
a_{20}					-30.62175	-1.71234
a_{21}					-0.07887	0.27886
a_{22}						0.88715
a_{23}						-0.67662
a_{24}						0.04349
a_{25}						-0.38525
Q_r	147963.94	147964.49	147964.1	147962.72	147963.53	147963.15
R_1	0.00162	0.00029	0.00123	0.00210	0.00068	0.00034
C_1	0.06704	0.02097	0.02714	0.06499	0.02596	0.05867
R_2	0.00053	0.00125	8.86633E-05	0.00011	0.00091	0.00156
C_2	0.05142	0.03845	0.03241	0.04186	0.072524062	0.04877
MOF	0.00775	0.00764	0.00764	0.00783	0.00765	0.00766
Calculation Time (sec)	357.12	392.86	426.73	461.535	501.15	539.81

Table 5: Optimal parameters based on several algorithms for Case 2

	EA	FBI	GWO	PSO	BSA
Ro	0.000568	0.000719	0.002335	0.00001	0.000588
a_0	3.748055	2.635103	3.644386	5	2.44061
a_1	0.365885	-0.38412	-0.00064	-1.0927	13.09921
a_2	-3.0791	1.030771	-46.5625	0.394574	-9.06146
a_3	-0.2624	0.090911	-0.29748	100	-13.4491
a_4	-14.4221	0.131675	-7.09734	-100	-34.0529
a_5	0.134894	0.367197	0.833493	0.094509	-1.96034
a_6	-10.8373	-0.33207	-12.1331	-100	-97.1077
a_7	-0.1236	0.762054	-0.16797	-0.97144	15.44068
a_8	-1.58334	0.336337	-38.5273	-100	-27.0616
a_9	-0.06919	0.359072	-0.3547	0.14212	-7.11499
a_{10}	0.738454	-0.32747	-57.1836	-100	-72.6671
a_{11}	0.022825	0.355903	0.098728	-0.0308	-6.20173
a_{12}	-3.28428	-10.8378	-99.4059	-100	-55.0202
a_{13}	-0.16269	-1.16718	19.04225	-100	33.63797
Q_r	147964.2	147876.7	147949.6	170000	149654.8
R_1	0.000954	0.001705	6.11E-06	0.000001	0.004249
C_1	0.036197	0.059723	0.047881	0.1	0.088662
R_2	0.000946	0.000169	3.37E-06	0.000001	0.02417
C_2	0.059282	0.059705	0.017428	0.000001	0.079619
MOF	0.007654	0.009216	0.008614	0.097418	0.577422

4.4. Comparison of several optimization algorithms in Consideration of Non-Linear relation between V_{OC} and SOC

In this subsection, several recent optimization algorithms are applied to show the capability and robustness of the proposed EA in consideration of Non-Linear relation between V_{OC} and SOC. Beside the EA, 2020, the compared algorithms are Forensic-based investigation algorithm (FBI), 2020 [50], grey wolf optimizer GWO, 2021 [51], efficient particle swarm optimization (PSO), 1995, backtracking search algorithm (BSA), 2013 [52]. These algorithms are applied with the same number of individuals of 100 and maximum number of iterations of 500. Their obtained parameters and results are tabulated in Table 5. This table elucidates the high capability of the proposed EA in finding the global minimal as it obtains the minimum MOF with 0.007654 where GWO, FBI, PSO and BSA acquire 0.008614, 0.009216, 0.00974, and 0.5774, respectively. Furthermore, a robustness test for these algorithms is executed by running them 10 times and recording the Best, Mean, Worst, and standard deviation (Std) in Table 5. It is clear that the proposed EA is distinguished with high robustness minimum indices, Best, Mean, Worst, and Std, of 0.007654, 0.00861, 0.011873, and 0.001248, respectively.

For any meta- heuristic optimization method, there really is no promise to say that

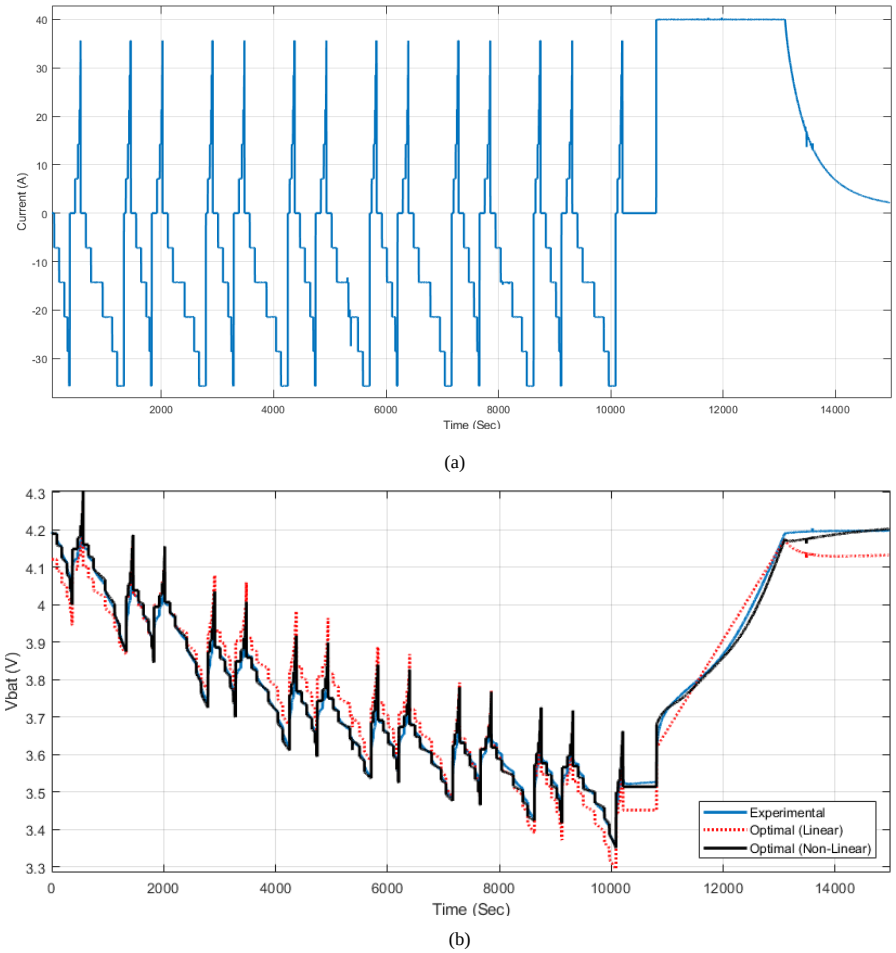

Figure 7: (a) Laboratory current profile with 150 km ARTEMIS driving cycle (b) Experimental and modeling responses of battery voltage

the gained response is the optimal option except it is identified [53]. This returns to the probability of such optimization methods to be trapped in a local optima and, subsequently, stop developing. As described in [44], the continuity in developing the best solution in the convergence curve declares a good indicator for avoiding local minimal area. Fig. 8 describes the EAâs convergence curve of ten separate runs. This figure demonstrates the significant development of the best solution by non-stick iterations at a local minimum. Added to that, Fig. 9 illustrates the box and Whiskers plot for the competitive optimization algorithms, MPO, FBI, GWO and EA, which demonstrates the high effectiveness of the EA in finding the minimum MOF compared with the others. Furthermore, a robustness test for these algorithms is executed by running them 10 times and recording the Best, Mean, Worst, standard deviation (Std) and the computation time per iterationin Table 6. It is clear that the proposed EA is distinguished with high robustness minimum indices, Best, Mean, Worst, and Std, of 0.007654, 0.00861, 0.011873, and 0.001248, respectively. In terms of

Table 6: Robustness test of several optimizers for Case 2

	EA	FBI	GWO	PSO	BSA
Best	0.007654	0.009216	0.008614	0.097418	0.577422
Mean	0.00861	0.01084	0.019526	0.556035	1.272247
Worst	0.011873	0.013717	0.026385	1.150793	2.879003
Std	0.001248	0.001342	0.006806	0.452099	0.757069
Time/Iteration (sec)	0.6048	1.2069	0.5716	0.7507	0.9980

the computation time per iteration, the proposed EA consumes 0.6048 sec compared with FBI, GWO, PSO and BSA which consume 1.2069 sec, 0.5716 sec, 0.7507 sec and 0.998 sec, respectively. It is cleared that the fast optimizer is GWO then the proposed EA.

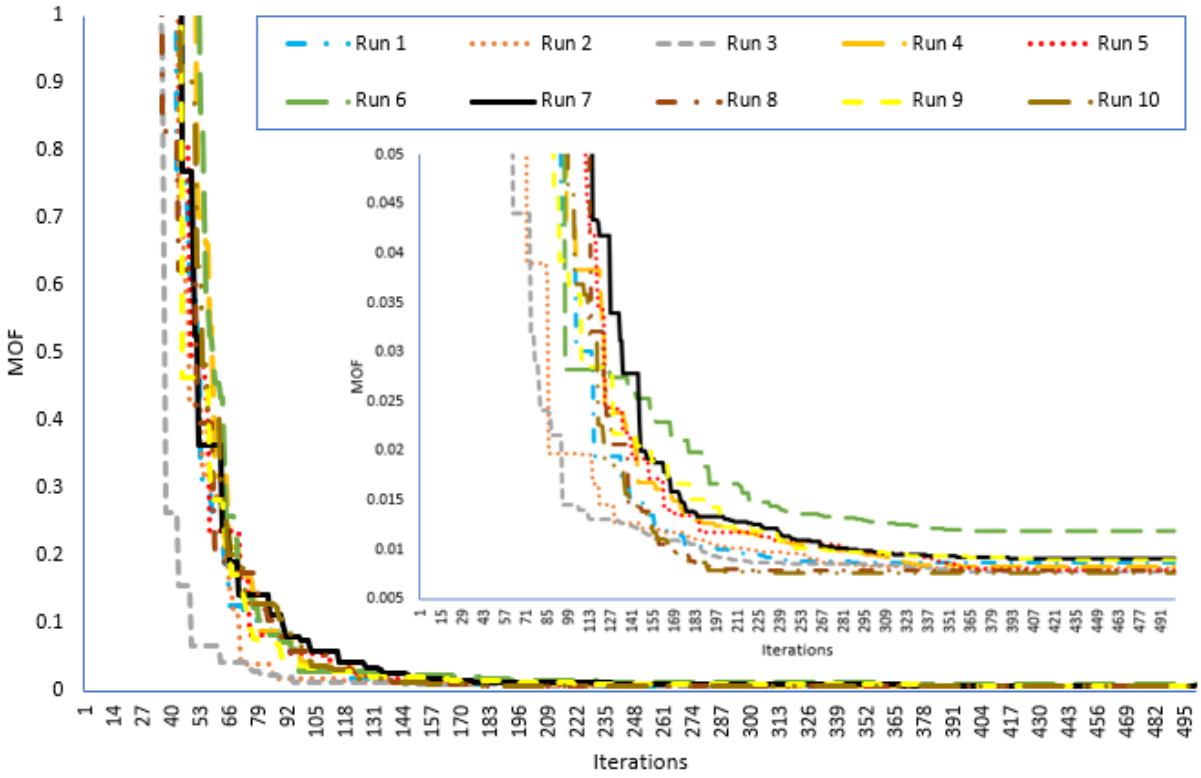

Figure 8: Convergence curve of the employed EA for Case 1

The EA employed is defined by its adaptive framework. However, there seem to be the size of the population (Ps) and the maximum number of iterations show high effect on results.

4.5. Parameter Tuning of Competitive Algorithms

In this subsection, the all competitive parameters are adjusted based on Taguchi's design of experiment approach, which reduces computational time and the number of experiments

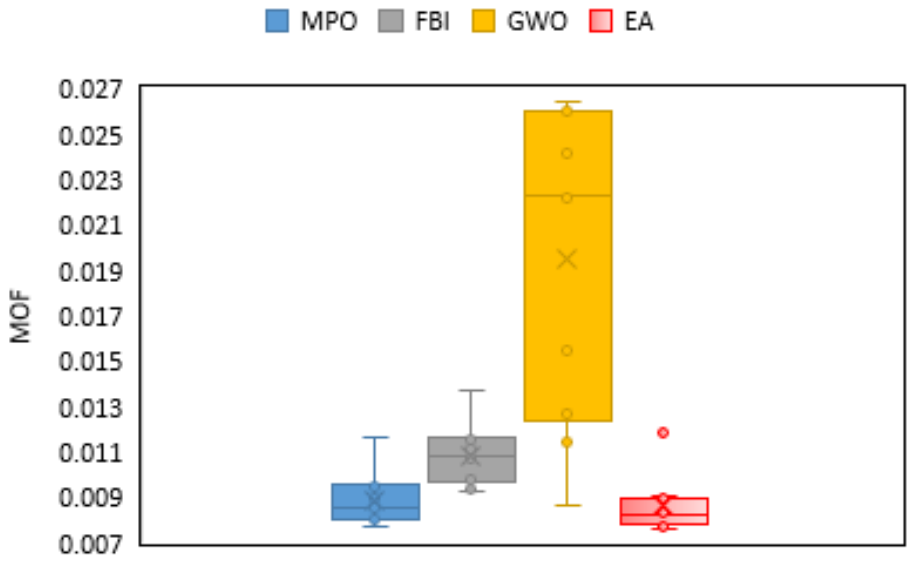

Figure 9: Box and Whiskers plot for MPO, FBI, GWO and EA for Case 1

Table 7: Combination of parameters for the compared algorithms

Parameters	Level 1	Level 2	Level 3
Population Size	25	50	100
Maximum number of iterations	100	300	500

required to get the optimum possible parameter arrangement [54]. The orthogonal array LÉ¡(32) is used to execute the parameter combinations listed in Table 7, as the number of parameters is 2 and each one has 3 levels. The array results in 9 treatments. Table 8 shows the orthogonal array with the MOF value.

Table 9 tabulates and depicts the response score and meaningful ranking of the parameters. The maximum number of iterations, rated first, has a significant impact on the performance of the EA in minimizing the MOF value, followed by the population size, ranked second. As a result, the following arrangement from Fig. 10 is chosen: The population size is set to 100, and the maximum number of iterations is set to 500. Similarly, for each of the examined methods, the parameter determination curves by means of the Taguchi methodology are depicted in Figs. 4.5 and 12. Similar conclusions may be derived, as the optimum tuning settings are supplied where the population size is set to 100, and the maximum number of iterations is set to 500. For the PSO, two other control parameters must be specified whereas the cognitive and social learning factors are required. Considering the maximum number of iterations is fixed at 500, Taguchi method is applied where the orthogonal array LÉ¡(33) is used to execute the parameter combinations and it is reduced to 8 treatments as the number of parameters is 3 and each one has 3 levels as listed in Table 10. Thus, the best values of the cognitive and social learning factors are 2 and 2, respectively.

Table 8: Orthogonal table based on Taguchi method for the compared algorithms

Population Size	Maximum number of iterations	MOF
25	100	0.023716523
25	300	0.00783557
25	500	0.007732807
50	100	0.007966795
50	300	0.000768923
50	500	0.0007697034
100	100	0.007732807
100	300	0.007697034
100	500	0.0007653744

Table 9: Response table of means for the EA.

Item	Population Size	Maximum number of iterations
Level 1	0.01309496667	0.01313870833
Level 2	0.0031684738	0.005433842333
Level 3	0.005398405133	0.003089294933
Delta	0.009926492869	0.0100494133970
Rank	2	1

Table 10: Combination of parameters for the PSO

Parameters	Level 1	Level 2	Level 3
Population Size	25	50	100
Cognitive learning factor	1	2	4
Social learning factor	1	2	4

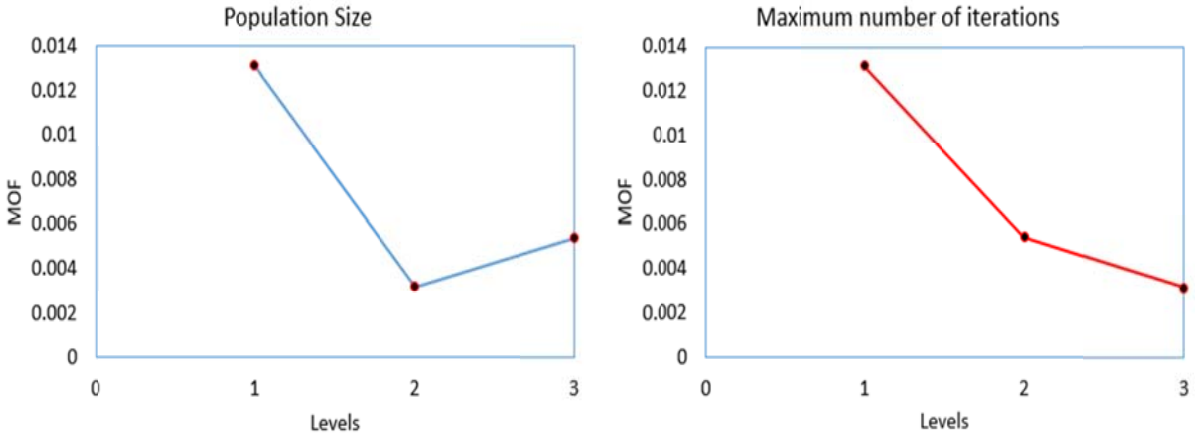

Figure 10: Parameters selection for EA based on Taguchi method

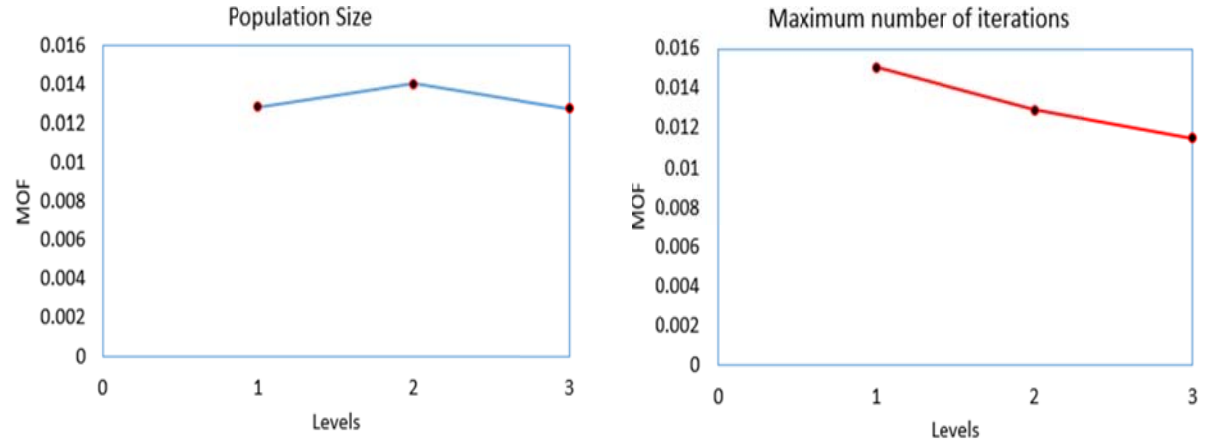

(a) FBI

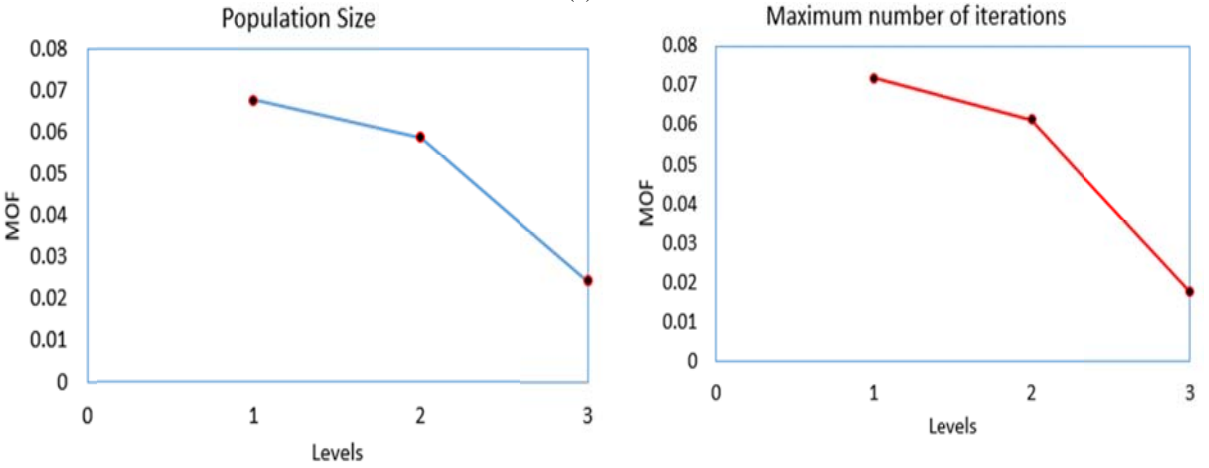

(b) GWO

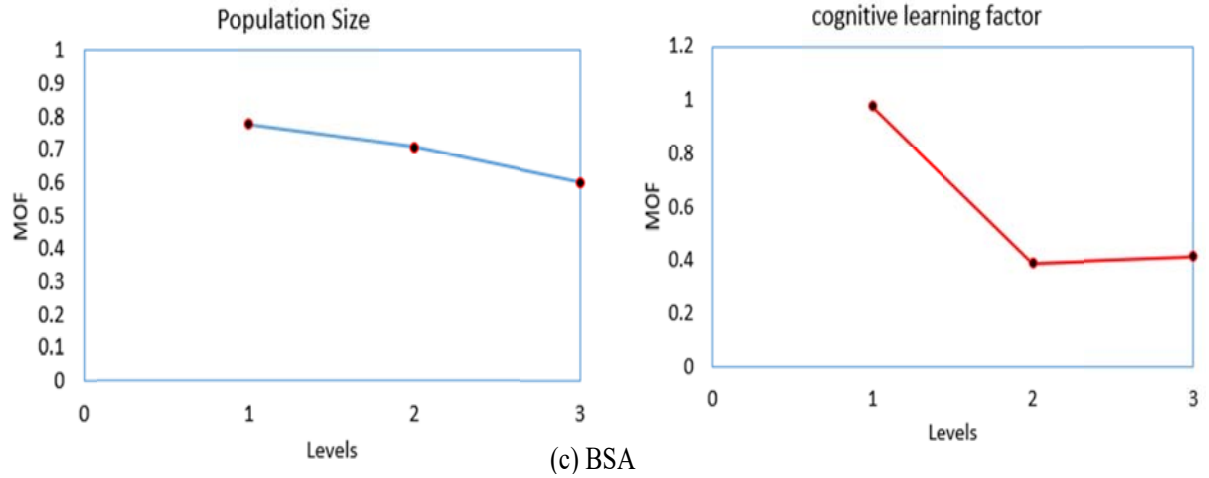

(c) BSA

Figure 11: Parameters selection based on the Taguchi method for FBI, GWO and BSA methods

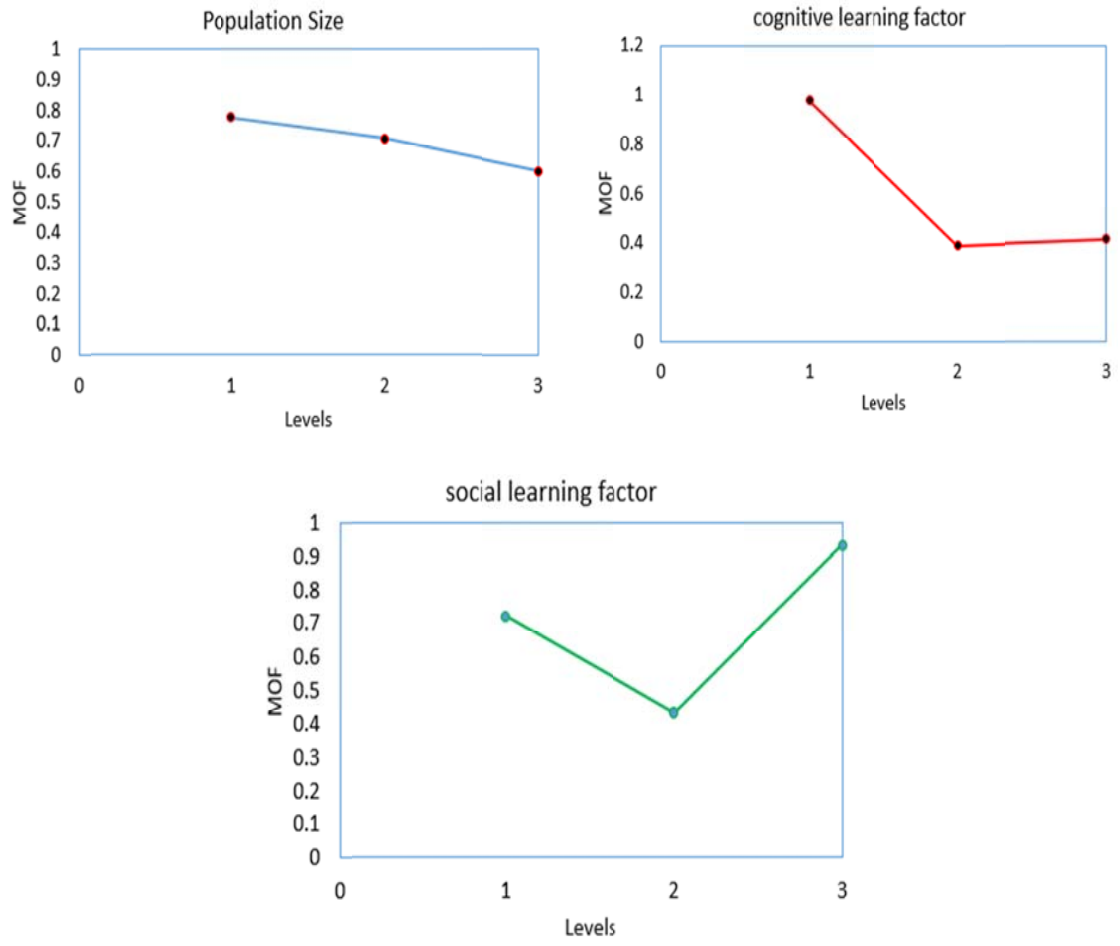

Figure 12: Parameters selection based on the Taguchi method for PSO method

5. DESIGN OF EXPERIMENTS

In this paper, the design of experimental tests is dependent on classification constraints. The objective aims at reducing the cycling times with preserving the important test features, such as the maximum current intensity and the amount of charge exchanged [55], [56]. The ARTEMIS driving cycle is selected for extracting the battery parameters using a dynamics model of the urban electric vehicle (BollorÃ© Bluecar).

5.1. Driving cycle

Recently, several normalized/non-normalized driving cycles are suggested to evaluate the pollution emissions and fuel consumption of gasoline-powered engines for examples the ECE, NEDC, UDC, ARTEMIS, FTP75,WLTC and NYCC [57]. The modeling of the tested driving cycle is employed based on speed-time sequences that emulates the traffic conditions and driving behavior in a specific area. In this paper, the Assessment and Reliability of Transport

Emission Models Inventory Systems (ARTEMIS) driving cycle is chosen for its real-world driving behavior. ARTEMIS has three driving cycles called urban, rural and highway. In this work, the ARTEMIS cycle selected to represent the urban and the rural cycle. Recently, various types of batteries have been developed to meet the main requirements of electric and hybrid vehicles with enhancing the drive performance and high reliability such as a commercial 40 Ah Li-ion battery [8] and [48], . This battery under reference of HED-SLPB90216216 that is produced by Kokam manufacturer is selected study.

5.2. Verification study on Artemis driving cycle

The ARTEMIS, Assessment and Reliability of Transport Emission Models Inventory Systems, driving cycle is generally represented in terms of their speed-time sequences which are originally based on the driving behavior and traffic conditions in a particular area. In the current paper, this driving cycle is performed by the urban and the rural cycle with the average distance of 22 km in 2075 seconds. The average and maximal speeds are 38.4 and 111.5 km/h, respectively. The proposed EA is applied to optimally identify the battery parameters considering the linear and non-linear relation between V_{OC} and the SOC as described in the previous sections. For both cases, Table 11 shows the obtained optimal parameters and their corresponding results. Similar conclusion is drawn where the linear consideration is unsuitable that it creates bad accuracy compared to the non-linearity relation. The considered objective, in the non-linear form, is greatly minimized to 0.00445 compared to 0.012 in the linear form. The root mean square of the normalized deviation between the estimated and experimental battery voltage is reduced from 0.0119 to 0.00437. Fig. 13 displays the error response of the battery voltage for both models. As shown,

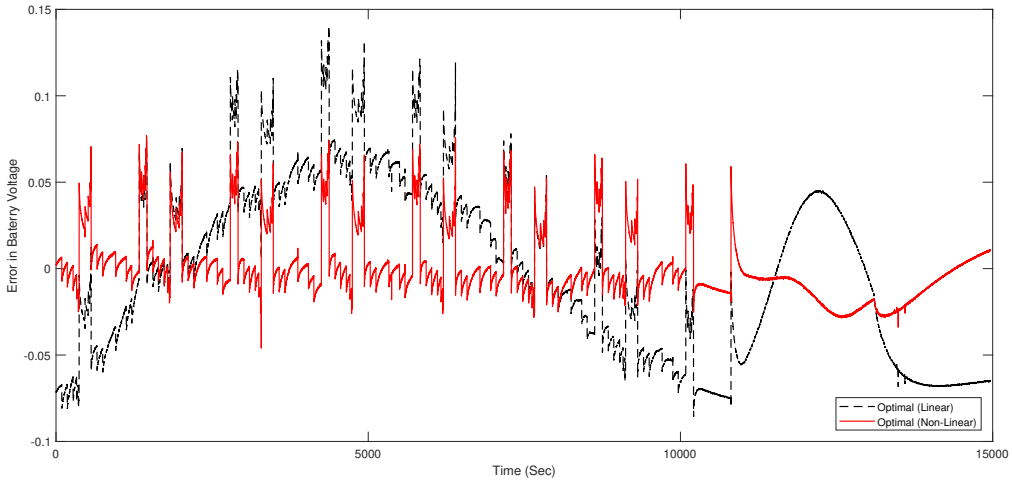

Figure 13: Error response of the battery voltage

very small error is clearly illustrated over the time where the maximum error does not exceed 0.07 for the non-linear model while it is reached to more than 0.13 several times

for the linear model. This improvement is originally due the accurate high non-linearity consideration between the open circuit voltage and the state of charge as shown in Fig. 14. This figure clearly illustrates the curved relationship in the non-linear model that makes accurate tracking to the experimental battery voltage. On the other side, no significant

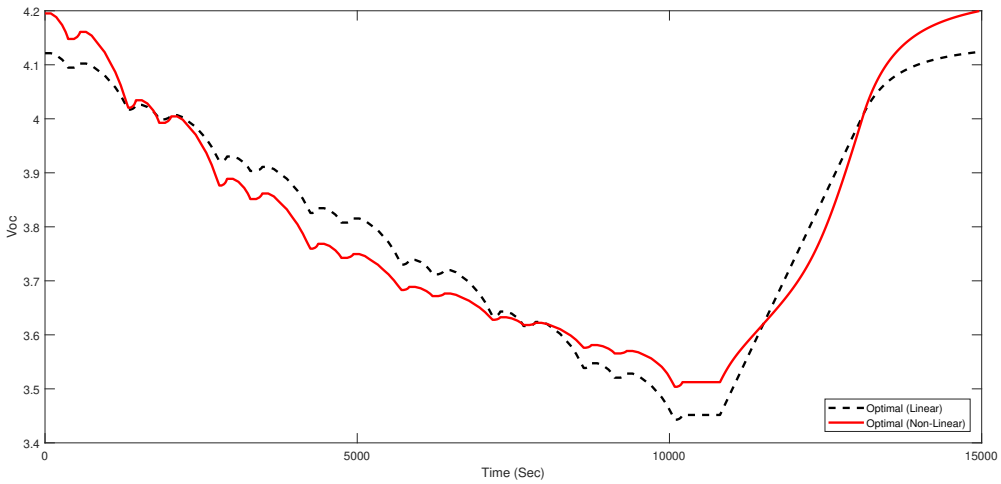

Figure 14: Response of the open circuit voltage for ARTEMIS driving cycle

preference of both models on the second objective of the root mean square of the normalized deviation between estimated and experimental state of charge as shown in Figs. 15 and 16 depicts the error response of the state of charge, respectively. From these figures, both models demonstrate the high accuracy in tracking the state of charge.

5.3. Efficient simplified nonlinear model of lithium-ion battery

A linear model of lithium-ion battery has been proposed in [8], this model is quite simple but it couldn't give precise identification because it doesn't take into account the nonlinear dynamics of the lithium-ion battery. The nonlinear model of lithium-ion battery presented in [49] is efficient but it is too complicated and requires more computation time to identify its parameters and to estimate the SoC. The proposed simplified model is presented with keeping the same performance obtained in [49]. This reduced model contains only 5 parameters instead of 13 as it can be shown in Table 1. The proposed model is compared with 13^{th} parameter to show their performance. The obtained results are shown by Figs. 17 and 18 As shown, no significant difference is noticed between both models in evaluating the battery voltage and the state of charge. Furthermore, the simplified model (N=5) has less computational time than the high accurate one of (N=13) since the simplified model has 16.31% decrease in the computation time.

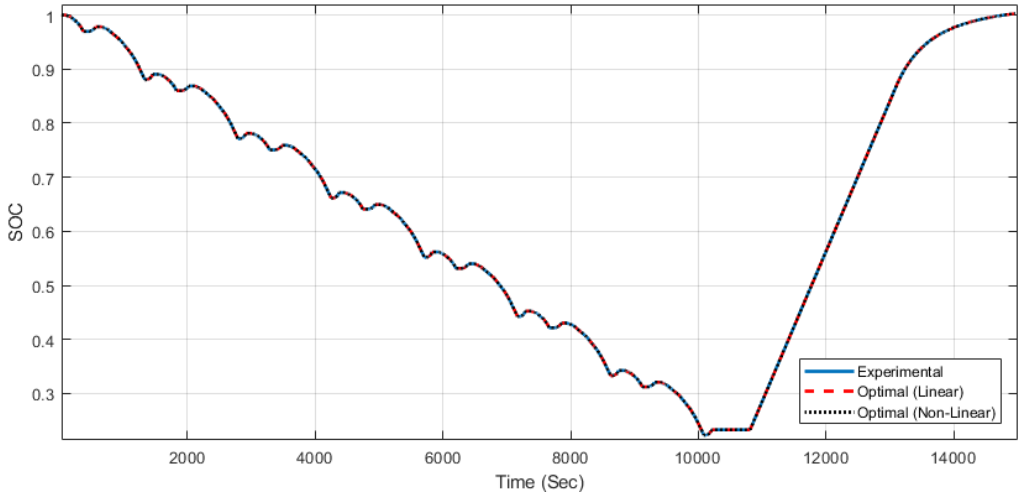

Figure 15: State of charge experimental and modeling responses

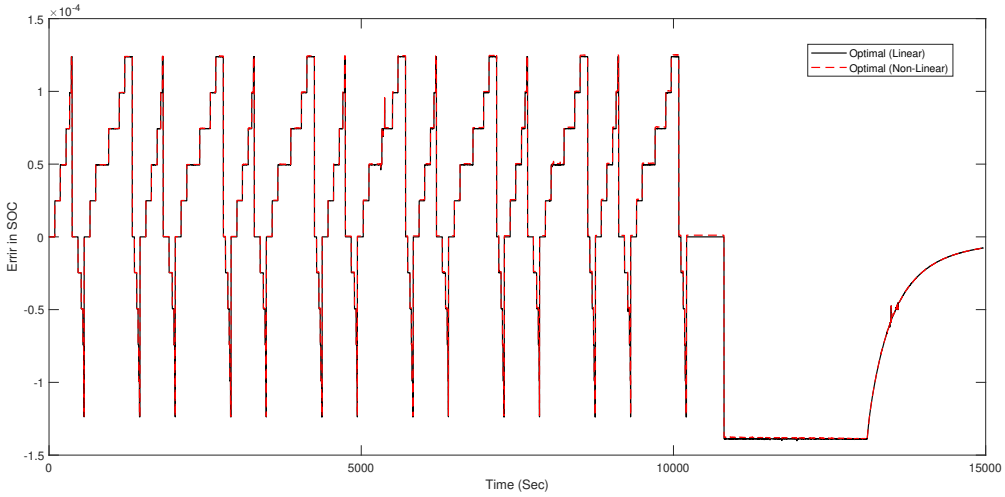

Figure 16: Error response of the state of charge for ARTEMIS cycle

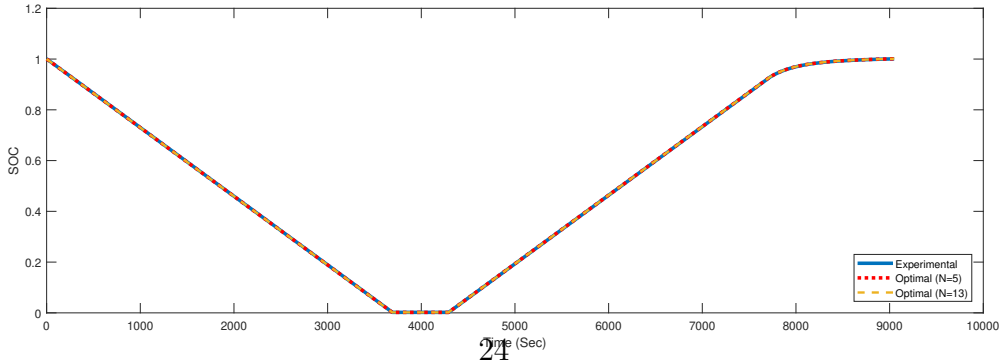

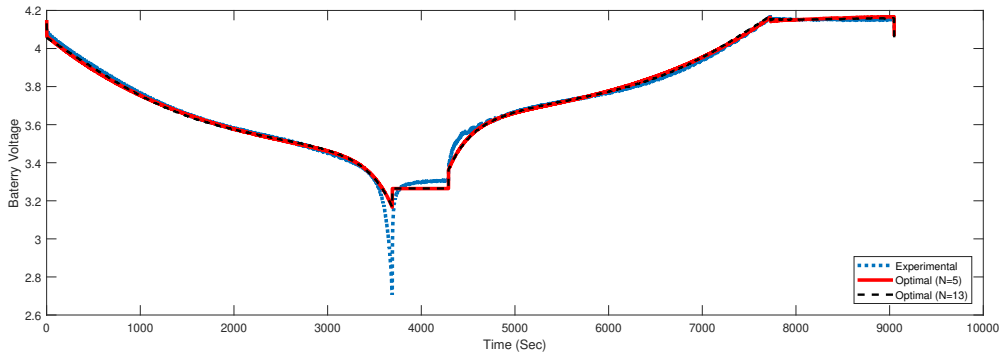

Figure 17: Comparison between 5^{th} and 13^{th} parameters models

Figure 18: Comparison between 5^{th} and 13^{th} parameters models for ARTEMIS cycle

6. Conclusion and future work

6.1. Conclusion

An improved procedure for lithium ion battery parameter estimation has been proposed in this paper based on an enhanced equilibrium optimization algorithm. The significant contributions can be concluded as follows:

- A good compromise between state space model and nonlinear model is obtained and the estimation problem is divided into three steps that enhance the solution methodology and find the accurate relation for each stage.
- An assessment between various non-linear models, to represent the dependency between open circuit voltages and the battery state of charge, has been employed compared with linear models.
- An enhanced equilibrium optimization algorithm considering has been employed, the statistical indices reflect that the proposed method improve the accuracy by 12% compared to competitive methods.
- Comparison with other state-of-the-art solutions have shown that the proposed give more precise results with less computation time (16 % improvement).
- Dynamic verification study has been carried out on ARTEMIS driving cycle to prove the capability of the proposed solution.
- Tuning the parameters of all competitive algorithms to assign the optimal modeling method at the best algorithm parameters.

Table 11: Optimal parameters based on EA for Linear and Non-Linear relation for ARTEMIS driving cycle

Parameter	Linear	Non-Linear (N=5)	Non-Linear (N=13)
R (mΩ)	0.002334072394	0.0003068363818	0.00131930343899999
R_1 (Ω))	0.001244251137	0.00037837	0.001630968
C_1 (F)	0.08266382139	0.06375762	0.019172327
R_2 (Ω))	0.0006059282676	0.003494296	0.001234919
C_2 (F)	0.068005188	0.099650938	0.032159331
Q_r (As)	144000	143999.998	144000.234499999
Coefficients	b_0 3.248043 b_1 0.873431	a_0 3.40327 a_1 0.80028 a_2 -2.3124 a_3 -33.35991 a_4 -30.68399 a_5 -46.75711	a_0 3.33767 a_7 -1.16956 a_1 0.27462 a_8 -24.78047 a_2 -4.77465 a_9 0.34301 a_3 -0.24291 a_{10} -0.87348 a_4 -5.25495 a_{11} 0.65556 a_5 0.23610 a_{12} -58.29117 a_6 -14.74987 a_{13} 13.48667
F1	0.01192552947	0.004577236303	0.004378931369
F2	0.000077476147	0.00007747614742	0.00007747937708
MOF	0.01200300562	0.00465471245	0.004456410746
Calculation time (sec)	584.15	668.22	842.371

6.2. Future work

The future trends of this study can be classified into two main categories:

- Considering the thermal impacts for single battery or a set of batteries especially for varied environmental conditions and for electrical vehicles applications.
- Considering the uncertainty of measurements and the shift noises from sensors and the battery aging.
- Developing new solution modeling for real time applications of the different types of batteries

ACKNOWLEDGMENT

This work was supported by Taif University Researchers Supporting Project number (TURSP-2020/86), Taif University, Taif, Saudi Arabia.

References

[1] B. Rowden and N. Garcia-Araez, "Estimating lithium-ion battery behavior from half-cell data," *Energy Reports*, vol. 7, pp. 97–103, 2021, sI: 5th AC-CDTESA.

[2] A. A. Abou El-Ela, R. A. El-Seheimy, A. M. Shaheen, W. A. Wahbi, and M. T. Mouwafi, "Pv and battery energy storage integration in distribution networks using equilibrium algorithm," *Journal of Energy Storage*, vol. 42, p. 103041, 2021.

[3] A. R. Ginidi, A. M. Shaheen, R. A. El-Sehiemy, and E. Elattar, "Supply demand optimization algorithm for parameter extraction of various solar cell models," *Energy Reports*, vol. 7, pp. 5772–5794, 2021.

[4] R. Xiong, J. Wang, W. Shen, J. Tian, and H. Mu, "Co-estimation of state of charge and capacity for lithium-ion batteries with multi-stage model fusion method," *Engineering*, 2021.

[5] Z. Yuan, W. Wang, H. Wang, and N. Razmjooy, "A new technique for optimal estimation of the circuit-based pemfcs using developed sunflower optimization algorithm," *Energy Reports*, vol. 6, pp. 662–671, 2020.

[6] M. de Fatima Brondani, A. T. Z. R. Sausen, P. S. Sausen, and M. O. Binelo, "Parameter estimation of lithium ion polymer battery mathematical model using genetic algorithm," *Computational and Applied Mathematics*, vol. 37, no. 1, pp. 296–313, 2018.

[7] M. Brondani, A. T. Z. R. Sausen, P. S. Sausen, and M. O. Binelo, "Battery model parameters estimation using simulated annealing," *TEMA (São Carlos)*, vol. 18, no. 1, pp. 127–137, 2017.

[8] R. A. El-Sehiemy, M. Hamida, and T. Mesbahi, "Parameter identification and state-of-charge estimation for lithium-polymer battery cells using enhanced sunflower optimization algorithm," *International Journal of Hydrogen Energy*, vol. 45, no. 15, pp. 8833 – 8842, 2020.

[9] Z. Wei, G. Dong, X. Zhang, J. Pou, Z. Quan, and H. He, "Noise-immune model identification and state of charge estimation for lithium-ion battery using bilinear parameterization," *IEEE Transactions on Industrial Electronics*, pp. 1–1, 2020.

[10] L. Sun, G. Li, and F. You, "Combined internal resistance and state-of-charge estimation of lithium-ion battery based on extended state observer," *Renewable and Sustainable Energy Reviews*, vol. 131, p. 109994, 2020.

[11] L. Zhao, Z. Liu, and G. Ji, "Lithium-ion battery state of charge estimation with model parameters adaptation using hâ extended kalman filter," *Control Engineering Practice*, vol. 81, pp. 114 – 128, 2018.

[12] B. Ning, B. Cao, B. Wang, and Z. Zou, "Adaptive sliding mode observers for lithium-ion battery state estimation based on parameters identified online," *Energy*, vol. 153, pp. 732 – 742, 2018.

[13] Q. Yu, R. Xiong, C. Lin, W. Shen, and J. Deng, "Lithium-ion battery parameters and state-of-charge joint estimation based on h-infinity and unscented kalman filters," *IEEE Transactions on Vehicular Technology*, vol. 66, no. 10, pp. 8693–8701, 2017.

[14] X. Hu, D. Cao, and B. Egardt, "Condition monitoring in advanced battery management systems: Moving horizon estimation using a reduced electrochemical model," *IEEE/ASME Transactions on Mechatronics*, vol. 23, no. 1, pp. 167–178, 2018.

[15] M. Li, "Li-ion dynamics and state of charge estimation," *Renewable Energy*, vol. 100, pp. 44 – 52, 2017, special Issue: Control and Optimization of Renewable Energy Systems.

[16] J. Meng, M. Boukhnifer, and D. Diallo, "Comparative study of lithium-ion battery open-circuit-voltage online estimation methods," *IET Electrical Systems in Transportation*, vol. 10, no. 2, pp. 162–169, 2020.

[17] M. Hannan, M. Lipu, A. Hussain, and A. Mohamed, "A review of lithium-ion battery state of charge estimation and management system in electric vehicle applications: Challenges and recommendations," *Renewable and Sustainable Energy Reviews*, vol. 78, pp. 834 – 854, 2017.

[18] R. Xiong, J. Tian, H. Mu, and C. Wang, "A systematic model-based degradation behavior recognition and health monitoring method for lithium-ion batteries," *Applied Energy*, vol. 207, pp. 372 – 383, 2017, transformative Innovations for a Sustainable Future â Part II. [Online]. Available: http://www.sciencedirect.com/science/article/pii/S0306261917306645

[19] X. Hu, H. Jiang, F. Feng, and B. Liu, "An enhanced multi-state estimation hierarchy for advanced lithium-ion battery management," *Applied Energy*, vol. 257, p. 114019, 2020. [Online]. Available: http://www.sciencedirect.com/science/article/pii/S0306261919317064

[20] I. M. Safwat, W. Li, and X. Wu, "A novel methodology for estimating state-of-charge of li-ion batteries using advanced parameters estimation," *Energies*, vol. 10, no. 11, p. 1751, 2017.

[21] F. Yang, W. Li, C. Li, and Q. Miao, "State-of-charge estimation of lithium-ion batteries based on gated recurrent neural network," *Energy*, vol. 175, pp. 66 – 75, 2019.

[22] L. Hu, X. Hu, Y. Che, F. Feng, X. Lin, and Z. Zhang, "Reliable state of charge estimation of battery packs using fuzzy adaptive federated filtering," *Applied Energy*, vol. 262, p. 114569, 2020.

[23] K. V. Singh, H. O. Bansal, and D. Singh, "Hardware-in-the-loop implementation of anfis based adaptive soc estimation of lithium-ion battery for hybrid vehicle applications," *Journal of Energy Storage*, vol. 27, p. 101124, 2020.

[24] G. O. Sahinoglu, M. Pajovic, Z. Sahinoglu, Y. Wang, P. V. Orlik, and T. Wada, "Battery state-of-charge estimation based on regular/recurrent gaussian process regression," *IEEE Transactions on Industrial Electronics*, vol. 65, no. 5, pp. 4311–4321, 2018.

[25] J. Chen, Q. Ouyang, C. Xu, and H. Su, "Neural network-based state of charge observer design for lithium-ion batteries," *IEEE Transactions on Control Systems Technology*, vol. 26, no. 1, pp. 313–320, 2018.

[26] Q. Wang, Z. Wang, L. Zhang, P. Liu, and Z. Zhang, "A novel consistency evaluation method for series-connected battery systems based on real-world operation data," *IEEE Transactions on Transportation Electrification*, 2020.

[27] C. She, Z. Wang, F. Sun, P. Liu, and L. Zhang, "Battery aging assessment for real-world electric buses based on incremental capacity analysis and radial basis function neural network," *IEEE Transactions on Industrial Informatics*, vol. 16, no. 5, pp. 3345–3354, 2019.

[28] L. Zhang, X. Hu, Z. Wang, J. Ruan, C. Ma, Z. Song, D. G. Dorrell, and M. G. Pecht, "Hybrid electrochemical energy storage systems: An overview for smart grid and electrified vehicle applications," *Renewable and Sustainable Energy Reviews*, p. 110581, 2020.

[29] K. Liu, X. Hu, H. Zhou, L. Tong, D. Widanalage, and J. Macro, "Feature analyses and modelling of lithium-ion batteries manufacturing based on random forest classification," *IEEE/ASME Transactions on Mechatronics*, 2021.

[30] K. Liu, T. Ashwin, X. Hu, M. Lucu, and W. D. Widanage, "An evaluation study of different modelling techniques for calendar ageing prediction of lithium-ion batteries," *Renewable and Sustainable Energy Reviews*, vol. 131, p. 110017, 2020.

[31] Y. Zheng, W. Gao, M. Ouyang, L. Lu, L. Zhou, and X. Han, "State-of-charge inconsistency estimation of lithium-ion battery pack using mean-difference model and extended kalman filter," *Journal of Power Sources*, vol. 383, pp. 50 – 58, 2018.

[32] L. Chen, Z. Wang, Z. LÃ¼, J. Li, B. Ji, H. Wei, and H. Pan, "A novel state-of-charge estimation method of lithium-ion batteries combining the grey model and genetic algorithms," *IEEE Transactions on Power Electronics*, vol. 33, no. 10, pp. 8797–8807, 2018.

[33] V. Sangwan, R. Kumar, and A. K. Rathore, "Estimation of battery parameters of the equivalent circuit model using grey wolf optimization," in *2016 IEEE 6th International Conference on Power Systems (ICPS)*, 2016, pp. 1–6.

[34] T. Mesbahi, N. Rizoug, F. Khenfri, P. BartholomeÃ¼s, and P. Le Moigne, "Dynamical modelling and emulation of li-ion batteriesâsupercapacitors hybrid power supply for electric vehicle applications," *IET Electrical Systems in Transportation*, vol. 7, no. 2, pp. 161–169, 2017.

[35] A. Faramarzi, M. Heidarinejad, B. Stephens, and S. Mirjalili, "Equilibrium optimizer: A novel optimization algorithm," *Knowledge-Based Systems*, vol. 191, p. 105190, 2020.

[36] M. Abdel-Basset, V. Chang, and R. Mohamed, "A novel equilibrium optimization algorithm for multi-thresholding image segmentation problems," *Neural Computing and Applications*, pp. 1–34, 2020.

[37] H. Özkaya, M. Yıldız, A. R. Yıldız, S. Bureerat, B. S. Yıldız, and S. M. Sait, "The equilibrium optimization algorithm and the response surface-based metamodel for optimal structural design of vehicle components," *Materials Testing*, vol. 62, no. 5, pp. 492–496, 2020.

[38] A. S. Menesy, H. M. Sultan, and S. Kamel, "Extracting model parameters of proton exchange membrane fuel cell using equilibrium optimizer algorithm," in *2020 International Youth Conference on Radio Electronics, Electrical and Power Engineering (REEPE)*. IEEE, 2020, pp. 1–7.

[39] S. Agnihotri, A. Atre, and H. Verma, "Equilibrium optimizer for solving economic dispatch problem,"

in *2020 IEEE 9th Power India International Conference (PIICON)*. IEEE, pp. 1–5.
[40] A. M. Shaheen, A. R. Ginidi, R. A. El-Sehiemy, and S. S. M. Ghoneim, "A forensic-based investigation algorithm for parameter extraction of solar cell models," *IEEE Access*, vol. 9, pp. 1–20, 2021.
[41] Y. Gao, Y. Zhou, and Q. Luo, "An efficient binary equilibrium optimizer algorithm for feature selection," *IEEE Access*, vol. 8, pp. 140 936–140 963, 2020.
[42] D. T. Abdul-hamied, A. M. Shaheen, W. A. Salem, W. I. Gabr, and R. A. El-sehiemy, "Equilibrium optimizer based multi dimensions operation of hybrid AC/DC grids," *Alexandria Engineering Journal*, vol. 59, no. 6, pp. 4787–4803, dec 2020.
[43] K. Nusair and L. Alhmoud, "Application of equilibrium optimizer algorithm for optimal power flow with high penetration of renewable energy," *Energies*, vol. 13, no. 22, p. 6066, nov 2020.
[44] A. A. A. El-Ela, R. A. El-Sehiemy, A. M. Shaheen, and I. A. Eissa, "Optimal coordination of static VAR compensators, fixed capacitors, and distributed energy resources in egyptian distribution networks," *International Transactions on Electrical Energy Systems*, vol. 30, no. 11, sep 2020.
[45] X. Lai, W. Gao, Y. Zheng, M. Ouyang, J. Li, X. Han, and L. Zhou, "A comparative study of global optimization methods for parameter identification of different equivalent circuit models for li-ion batteries," *Electrochimica Acta*, vol. 295, pp. 1057 – 1066, 2019.
[46] S. Orcioni, L. Buccolini, A. Ricci, and M. Conti, "Lithium-ion battery electrothermal model, parameter estimation, and simulation environment," *Energies*, vol. 10, no. 3, p. 375, 2017.
[47] H. Rahimi-Eichi, F. Baronti, and M. Chow, "Online adaptive parameter identification and state-of-charge coestimation for lithium-polymer battery cells," *IEEE Transactions on Industrial Electronics*, vol. 61, no. 4, pp. 2053–2061, April 2014.
[48] A. Affanni, A. Bellini, G. Franceschini, P. Guglielmi, and C. Tassoni, "Battery choice and management for new-generation electric vehicles," *IEEE Transactions on Industrial Electronics*, vol. 52, no. 5, pp. 1343–1349, Oct 2005.
[49] T. Mesbahi, F. Khenfri, N. Rizoug, K. Chaaban, P. Bartholomeus, and P. L. Moigne, "Dynamical modeling of li-ion batteries for electric vehicle applications based on hybrid particle swarm-nelder-mead (pso-nm) optimization algorithm," *Electric Power Systems Research*, vol. 131, pp. 195 – 204, 2016.
[50] A. Shaheen, A. Elsayed, R. A. El-Sehiemy, and A. Y. Abdelaziz, "Equilibrium optimization algorithm for network reconfiguration and distributed generation allocation in power systems," *Applied Soft Computing*, vol. 98, p. 106867, jan 2021.
[51] A. M. Shaheen and R. A. El-Sehiemy, "Optimal coordinated allocation of distributed generation units capacitor banks voltage regulators by egwa," *IEEE Systems Journal*, vol. 15, no. 1, pp. 257–264, 2021.
[52] A. M. Shaheen and R. A. El-Sehiemy, "Enhanced feeder reconfiguration in primary distribution networks using backtracking search technique," *Australian Journal of Electrical and Electronics Engineering*, vol. 17, no. 3, pp. 196–202, jul 2020.
[53] A. A. Elsakaan, R. A. El-Sehiemy, S. S. Kaddah, and M. I. Elsaid, "An enhanced moth-flame optimizer for solving non-smooth economic dispatch problems with emissions," *Energy*, vol. 157, pp. 1063–1078, 2018.
[54] M. A. Hossain, R. K. Chakrabortty, M. J. Ryan, and H. R. Pota, "Energy management of community energy storage in grid-connected microgrid under uncertain real-time prices," *Sustainable Cities and Society*, vol. 66, p. 102658, 2021.
[55] N. Rizoug, R. Sadoun, T. Mesbahi, P. Bartholumeus, and P. LeMoigne, "Aging of high power li-ion cells during real use of electric vehicles," *IET Electrical Systems in Transportation*, vol. 7, no. 1, pp. 14–22, 2017.
[56] T. Mesbahi, N. Rizoug, P. Bartholomeus, R. Sadoun, F. Khenfri, and P. Le Moigne, "Dynamic model of li-ion batteries incorporating electrothermal and ageing aspects for electric vehicle applications," *IEEE Transactions on Industrial Electronics*, vol. 65, no. 2, pp. 1298–1305, Feb 2018.
[57] J. Torres, R. Gonzalez, A. Gimenez, and J. Lopez, "Energy management strategy for plug-in hybrid electric vehicles. a comparative study," *Applied Energy*, vol. 113, pp. 816 – 824, 2014.